Bioorganic & Medicinal Chemistry 16 (2008) 9937–9947

Contents lists available at ScienceDirect

Bioorganic & Medicinal Chemistry

journal homepage: www.elsevier.com/locate/bmc

Using an aryl phenanthroimidazole moiety as a conjugated flexible intercalator to improve the hybridization efficiency of a triplex-forming oligonucleotide

Amany M. A. Osman [†], Per T. Jørgensen, Niels Bomholt, Erik B. Pedersen [*]

Nucleic Acid Center, Department of Physics and Chemistry, University of Southern Denmark, Campusvej 55, DK-5230 Odense M, Denmark

ARTICLE INFO

Article history:
Received 19 May 2008
Revised 3 October 2008
Accepted 12 October 2008
Available online 17 October 2008

Keywords:
Intercalating nucleic acids
Phenanthroimidazole
DNA Triplex stability
Molecular modeling

ABSTRACT

When inserting 2-phenyl or 2-naphth-1-yl-phenanthroimidazole intercalators (**X** and **Y**, respectively) as bulges into triplex-forming oligonucleotides, both intercalators show extraordinary high thermal stability of the corresponding Hoogsteen-type triplexes and Hoogsteen-type parallel duplexes with high discrimination to Hoogsteen mismatches. Molecular modeling shows that the phenyl or the naphthyl ring stacks with the nucleobases in the TFO, while the phenanthroimidazol moiety stacks with the base pairs of the dsDNA. DNA-strands containing the intercalator **X** show higher thermal triplex stability than DNA-strands containing the intercalator **Y**. The difference can be explained by a lower degree of planarity of the intercalator in the case of naphthyl. It was also observed that triplex stability was considerably reduced when the intercalators **X** or **Y** was replaced by 2-(naphthlen-1-yl)imidazole. This confirms intercalation as the important factor for triplex stabilization and it rules out an alternative complexation of protonated imidazole with two phosphate groups. The intercalating nucleic acid monomers **X** and **Y** were obtained via a condensation reaction of 9,10-phenanthrenequinone (**4**) with (*S*)-4-(2-(2,2-dimethyl-1,3-dioxolan-4-yl)ethoxy)benzaldehyde (**3a**) or (*S*)-4-(2-(2,2-dimethyl-1,3-dioxolan-4-yl) ethoxy)-1-naphthaldehyde (**3b**), respectively, in the presence of acetic acid and ammonium acetate. The required monomers for DNA synthesis using amidite chemistry were obtained by standard deprotection of the hydroxy groups followed by 4,4′-dimethoxytritylation and phosphitylation.

1. Introduction

The ability of triplex-forming oligonucleotides (TFOs) to interact specifically with polypurine/polypyrimidine double-stranded DNA forming triplexes has shown them as candidates for regulation of transcription of genomic DNA in the so-called antigene strategy.[1–7] Moreover, TFOs induce gene recombination and repairing genetic defects in mammalian cells.[8–10] However, in many cases triplexes are thermodynamically less stable than corresponding duplexes. For this reason, an enormous number of oligodeoxynucleotides (ODN) have been developed, either by modifying the nucleobase,[11–13] the sugar part,[14–19] or the phosphate backbone[20–27] to improve triplex stabilization. The triplex stabilization can also be achieved by insertion of different intercalating agents. Recently, we observed the extraordinary stable Hoogsteen-type triplexes and duplexes, when the intercalator (*R*)-1-*O*-[4-(1-pyrenylethynyl) benzyl]- glycerol (**W**, TINA, Fig. 1) was inserted as a bulge in the middle of a TFO.[28]

The phenyl group of TINA is supposed to stack with the nucleobases in the TFO, while the pyrene moiety is expected to intercalate with the nucleobases of the duplex. In our search for triple-helix specific binding compounds that would function under physiological conditions; we have used the conjugated intercalator **W** to avoid self-association or quadruplex formation of G-rich oligonucleotides. Contrary to wild-type oligonucleotides, the corresponding oligonucleotides with **W** insertions were able to form stable triplexes in the presence of a physiologic potassium ion concentration.[29] However, polycyclic aromatic hydrocarbons such as phenanthrene and pyrene are carcinogenic environmental pollutants.[30] Therefore, the 1*H*-phenanthro[9,10-*d*]imidazol-2-yl group is worth considering to substitute the pyrenyl conjugated system of **W**. It has many desirable properties such as good stability, ease of introduction into molecular system containing an aromatic aldehyde, use as a chromophore with high extinction coefficient, readily tuneable absorption wavelength, and fluorophoric properties. More recently, 2-(phenyl or heterocyclic)-1*H*-phenanthro[9,10-*d*]imidazole has been reported as the inhibitor of microsomal prostaglandin E synthase-1 (mPGES-1) enzyme and it has been used for the treatment of various diseases, such

* Corresponding author. Tel.: +45 65502555; fax: +45 66158780.
E-mail address: ebp@ifk.sdu.dk (E.B. Pedersen).
† On leave from Chemistry Department, Faculty of Science, Menoufia University, Shebin El-Koam, Egypt.

0968-0896/$ - see front matter © 2008 Elsevier Ltd. All rights reserved.
doi:10.1016/j.bmc.2008.10.037

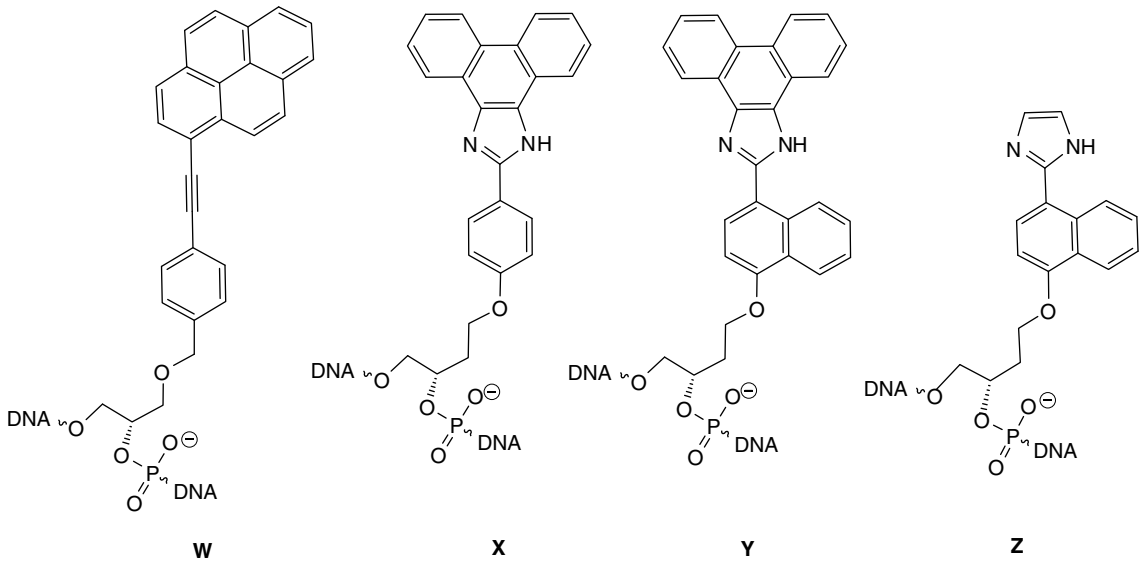

Figure 1. The synthesized intercalators **X**, **Y**, and **Z** with the reference intercalator **W** (TINA).

as osteoarthritis and rheumatoid arthritis.[31] The introduction of a fused imidazol ring with a larger aromatic system was believed to result in a higher affinity for dsDNA. In the present work, we describe the synthesis of two intercalating nucleic acids **X** and **Y** to enhance the stability of the TFO using a short flexible linker. The linker of the intercalators **X**, **Y**, and **Z** have the same number of atoms as the intercalator **W**, but for the ease of synthesis an oxygen atom and a carbon atom have been interchanged so that the oxygen is directly attached to the phenyl or the naphthyl ring. Thermal denaturation studies with the triplex-forming oligonucleotide proved that the intercalator **X** induced an enhanced triplex stability compared to wild type. From molecular modeling, it is found that intercalation is not necessarily the only possible explanation for triplex stabilization. The modeling showed also a possible active participation by a protonated imidazole ring which can have ionic interactions and form hydrogen bondings to two phosphate groups in two different backbones. However, the alternative mode of triplex stabilization was ruled out by synthesizing the truncated intercalator **Z** which gave less stable parallel triplexes, when inserted as a bulge.

2. Chemistry

The synthetic route toward the intercalating nucleic acid monomers (**6a,b**) is shown in Scheme 1. The key intermediates **3a**,**b** were synthesized from (*S*)-2-(2,2-dimethyl-1,3-dioxolan-4-yl)ethanol (**1**) by reaction with 4-hydroxybenzaldehyde (**2a**) or 4-hydroxy-1-naphthaldehyde (**2b**) under Mitsunobu conditions[32] (DEAD, THF, and Ph_3P) in high yields 81% and 92%, respectively (Scheme 1). Subsequent treatment of **3a**,**b** with phenanthrene-9,10-dione (**4**) and ammonium acetate in hot glacial acetic acid according to the procedure of Krebs and Spanggaard[33] afforded the monomers **6a**,**b**. When starting from **3a** the product mixture was separated by silica gel column chromatography to afford the deprotected (*S*)-4-(4-(1*H*-phenanthro[9,10-*d*]imidazol-2-yl)phenoxy)butane-1,2-diol (**6a**) in 72% yield and a minor amount of the corresponding diol (**5**) still protected with an isopropylidene group. Due to exchange of the imidazole protons, a line broadening was observed in the ^{1}H NMR spectrum of (**5**). This resulted in a broad singlet for the neighboring protons in the phenanthrene ring at C-4 and C-11. The corresponding compound (*S*)-4-(4-(1*H*-phenanthro[9,10-*d*]imidazol-2-yl)naphalen-1-yloxy)butane-1,2-diol (**6b**) was isolated fully deprotected by precipitation in 80% yield without chromatographic purification. The primary hydroxy group of compounds (**6a**,**b**) was protected by reaction with 4,4′-dimethoxytrityl chloride (DMT-Cl) in anhydrous pyridine at room temperature under a N_2 atmosphere. Silica gel purification afforded the DMT-protected compounds **7a**,**b** in 79% and 56% yield, respectively. The secondary hydroxy group of these compounds was phosphitylated overnight with 2-cyanoethyl *N*,*N*,*N*′,*N*′-tetraisopropyl phosphorodiamidite in the presence of diisopropyl ammonium tetrazolide as activator in anhydrous CH_2Cl_2 to afford **8a**,**b** in 86% and 81% yield, respectively (Scheme 1).

It was believed that the corresponding imidazolyl amidite derivative **13** without the phenanthrene ring system could be easily obtained from the corresponding monomer **10** (Scheme 2). In order to synthesize the monomer **10**, compound **3b** was deprotected with 80% aqueous acetic acid to give (*S*)-4-(3,4-dihydroxybutoxy)-1-naphthaldehyde (**9**) in 100% yield. This compound was reacted in ethanol and MeCN at 0 °C with a solution of 40% glyoxal in water and 20 M ammonium hydroxide overnight to afford (*S*)-4-(4-(1*H*-imidazol-2-yl)naphthalene-1-yloxy)butan-1,2-diol (**10**) in 44% yield in analogy with the procedure of Nakumura et al.[34] Unfortunately, the subsequent attempt to make the DMT-protected compound **12** failed although a variety of procedures were investigated. Therefore, it was decided to change the synthetic strategy. Instead, the primary hydroxyl group of compound **9** was DMT-protected to afford the compound **11** in 60% yield after purification by column chromatography. The imadazolyl derivative **12** was then obtained in 32% yield from compound **11** using the same reaction conditions as used for converting compound **9** into compound **10**. Finally, the amidite **13** was obtained in 81% yield by a standard phosphitylation reaction of compound **12**.

The obtained phosphoramidites **8a**,**b** and **13** were incorporated into a 14-mer oligonucleotide by a standard phosphoramidite protocol on an automated DNA synthesizer. However, an extended coupling time (10 min), in the oligonucleotide synthesis as was used for the amidite of the natural nucleosides. All modified ODNs were purified by reversed-phase HPLC, and confirmed by MALDI-TOF-MS analysis as reported in Section 7. The purity of the final sequences was determined by ion-exchange HPLC (IE-HPLC) to be more than 90%.

3. Thermal stability studies

The thermal stabilities of parallel triplexes and parallel duplexes as well as antiparallel DNA/DNA and DNA/RNA duplexes containing the intercalators **X**, **Y**, and **Z** were evaluated by thermal

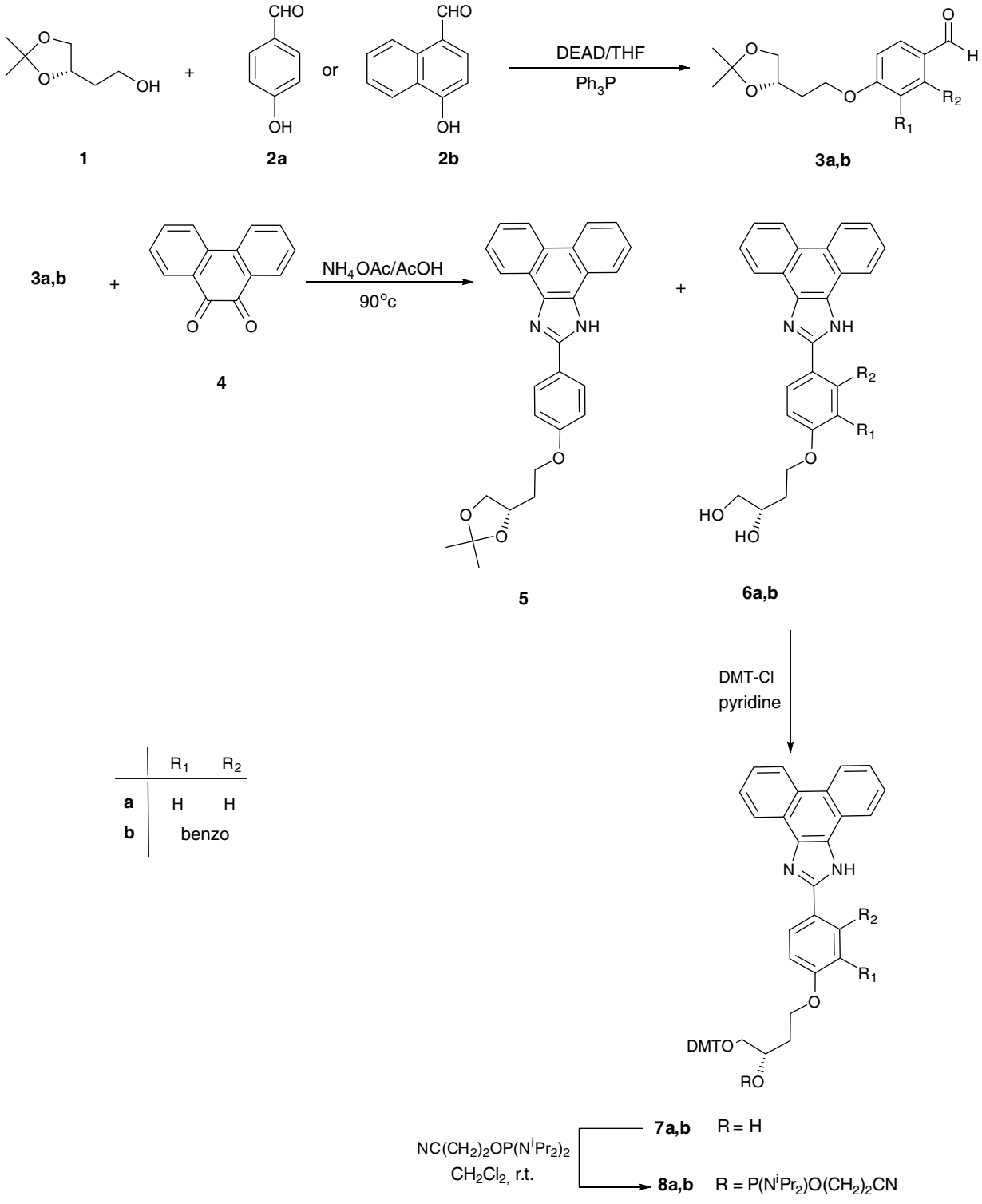

Scheme 1.

denaturation experiments. The thermal melting studies of **X** and **Y** were compared with the previously published data for the intercalator **W** (TINA)[28a] as shown in Tables 1–3. The melting temperatures (T_m, °C) were determined as the first derivatives of melting curves. Since protonation of cytosine is required to form stable Hoogsteen bonds, thermal stability of parallel triplexes using the synthesized oligonucleotides towards the duplex (**D1**)[35] was assessed both at pH 6.0 and pH 7.2, the ultimate goal being to find triplex formation at physiological pH conditions. Thermal stability of the corresponding parallel duplexes was also assessed using targeting to the purine strand **ON18**[36] (Table 1).

Stabilization of parallel triplexes was found in all cases when compared with the wild-type **ON1** at pH 6.0 and 7.2 except in case of **ON5** and **ON9** with insertion of the truncated intercalator **Z**. At pH 6.0, the stability of the modified sequences **ON10** and **ON13** with the intercalator **X** were also measured at a wavelength of $\lambda = 373$ nm, because of overlapping curves at $\lambda = 260$ nm for triplex and duplex melting. At pH 6 and independently of the site of inser-

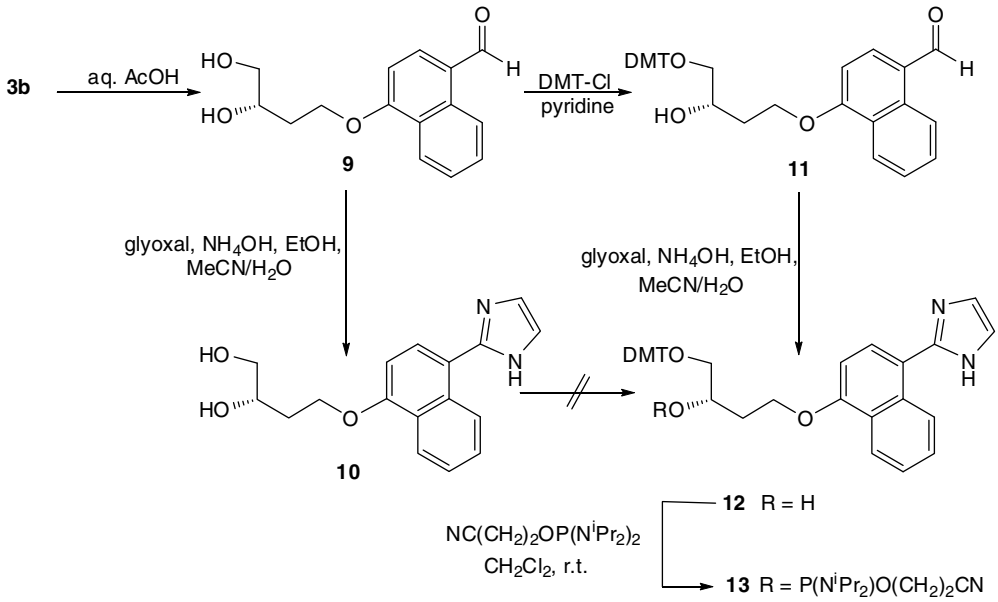

Scheme 2.

Table 1
T_m (°C) data for triplex and duplex melting, evaluated from UV melting curves (λ = 260 nm).

Entry	TFO	Parallel triplex[a] 3′-CTGCCCCTTTCTTTTTT 5′-GACGGGGAAAGAAAAAA (**D1**)			Parallel duplex[b] 5′-GACGGGGAAAGAAAAAA (**ON18**)
		pH 5.0	pH 6.0	pH 7.2	pH 6.0
ON1	5′-CCCCTTTCTTTTTT-3′	55.0[c]	28.0	<5.0	19.0
ON2	5′-CCCCTT**W**TCTTTTTT-3′	59.0[c]	45.5	28.0	33.5[c]
ON3	5′-CCCCTT**X**TCTTTTTT-3′	59.5	46.5	26.0	31.5
ON4	5′-CCCCTT**Y**TCTTTTTT-3′	55.0	40.5	18.5	21.5
ON5	5′-CCCCTT**Z**TCTTTTTT-3′	33.0	10.5	—[d]	—[d]
ON6	5′-CCCCTTTC**W**TTTTTT-3′	—[d]	39.5[c]	21.5[c]	30.0[c]
ON7	5′-CCCCTTTC**X**TTTTTT-3′	—[d]	43.5	25.0	34.5
ON8	5′-CCCCTTTC**Y**TTTTTT-3′	—[d]	35.5	18.5	23.0
ON9	5′-CCCCTTTC**Z**TTTTTT-3′	—[d]	13.5	—[d]	—[d]
ON10	5′-CCCCTTTCT**X**TTTTT-3′	—[d]	48.5[e]	33.5	31.5
ON11	5′-CCCCTTTCT**Y**TTTTT-3′	—[d]	38.5	18.5	19.5
ON12	5′-CCCCTT**W**TCT**W**TTTTT-3′	—[d]	56.5[c,e]	43.0[c]	38.0[c]
ON13	5′-CCCCTT**X**TCT**X**TTTTT-3′	—[d]	51.5[e]	37.0	37.5
ON14	5′-CCCCTT**Y**TCT**Y**TTTTT-3′	—[d]	46.5	15.0	20.5
ON15	5′-**W**CCCCTTTCTTTTTT-3′	—[d]	44.5[c]	20.5[c]	36.0[c]
ON16	5′-**X**CCCCTTTCTTTTTT-3′	—[d]	46.0	20.5	34.0
ON17	5′-CCCCTTTCTTTTTT**X**-3′	—[d]	43.5	20.0	31.5

[a] C = 1.5 μM of **ON1–17** and 1.0 μM of each strand of dsDNA(**D1**) in 20 mM sodium cacodylate, 100 mM NaCl, 10 mM $MgCl_2$, pH 5.0, pH 6.0, and 7.2. Duplex T_m = 58.5 °C (pH 6.0) and 57.0 °C (pH 7.2).
[b] C = 1.0 μM of each strand in 20 mM sodium cacodylate, 100 mM NaCl, 10 mM $MgCl_2$, pH 6.0.
[c] Data taken from Ref. 28a.
[d] Not determined.
[e] Third strand and duplex melting overlaid. T_m values determined at 373 nm.

tion of the intercaltor **X**, the triplex stabilities of **ON3/D1** (T_m = 46.5 °C), **ON7/D1** (T_m = 43.5 °C), and **ON10/D1** (T_m = 48.5 °C) are enormously increased compared to the unmodified triplex **ON1/D1** (T_m = 28.0 °C). The observed stabilization in the range of ΔT_m = 15.5–20.5 °C corresponds to an excellent intercalating system. When thermal melting using the insertions of **X** in **ON3** and **ON7** is compared with **W** in **ON2** and **ON6** almost identical triple stabilities are observed at pH 6.0 and 7.2 although with a small preference of **X** over **W** in three out of four cases. The opposite trend is observed upon double insertions when **ON12/D1** is compared with **ON13/D1**. This may reflect a stringent triplex structure which is highly selective toward intercalators on multiple insertions. Another interesting difference between the intercalators **W** and **X** was observed in annealing experiments where **X** gave a more clear annealing temperature upon cooling a mixture of **ON3** and **D1** (Fig. 2), than the one obtained for **ON2** and **D1**.

The importance of a large aromatic ring system as an intercalator was confirmed by observing that the truncated intercalator **Z** inserted as a bulge gave less stable parallel triplexes (**ON5** and **ON9**) when compared with the wild-type **ON1** at pH 5.0 and 6.0. As discussed later on under molecular modeling, an alternative ionic interaction between a protonated imidazole ring of the intercalator and the negative charged backbones of the triplex was found, which encouraged us to investigate thermal stability at pH 5.0 for the three novel intercalators. As can be seen from Table 1, a large decrease in thermal stability upon bulge insertion of intercalator Z (**ON5**) as compared to the wild-type (**ON1**) was detected. This observation confirms that the stability of the triplexes with bulge

Table 2
T_m (°C) data for mismatched Hoogsteen parallel triplex[a] melting, evaluated from UV melting curves (λ = 260 nm) at pH 6.0.

Entry	TFO	**D1**, **K** · **L** = T · A	**D2**, **K** · **L** = A · T	**D3**, **K** · **L** = C · G	**D4**, **K** · **L** = G · C
*Sequence 3′-CTGCCCCTT**K**CTTTTT*					
*5′-GACGGGGAA**L**GAAAAAA*					
ON1	5′-CCCCTTTCTTTTTT-3′	28.0	<5.0	<5.0	<5.0
ON2	5′-CCCCTT**W**TCTTTTTT-3′	45.5	27.0[b]	34.5[b]	28.5[b]
ON3	5′-CCCCTT**X**TCTTTTTT-3′	46.5	23.0	29.5	31.5
ON4	5′-CCCCTT**Y**TCTTTTTT-3′	40.5	16.5	21.0	25.5
ON10	5′-CCCCTTTCT**X**TTTTT-3′	48.5	30.5	33.0	35.5
ON11	5′-CCCCTTTCT**Y**TTTTT-3′	38.5	21.0	22.5	26.0
ON13	5′-CCCCTT**X**TCT**X**TTTTT-3′	51.5	35.5	37.0	42.0
ON14	5′-CCCCTT**Y**TCT**Y**TTTTT-3′	46.5	24.0	33.5	17.5

[a] C = 1.5 μM of each oligonucleotide and 1.0 μM of each strand of dsDNA in 20 mM sodium cacodylate, 100 mM NaCl, 10 mM $MgCl_2$, pH 6.0.
[b] Data taken from Ref. 28a.

Table 3
T_m (°C) data for Watson–Crick antiparallel duplexes melting, evaluated from UV melting curves (λ = 260 nm).

Entry	Sequences	DNA[a] 3′-GGGGAAAGAAAAAA (**ON19**)		RNA[b] 3′-r(GGGGAAAGAAAAAA) (**ON20**)
		pH 6.0	pH 7.2	pH 7.0
ON1	5′-CCCCTTTCTTTTTT-3′	49.5	49.5	52.0
ON2	5′-CCCCTT**W**TCTTTTTT-3′	46.5[c]	45.5[c]	–[d]
ON3	5′-CCCCTT**X**TCTTTTTT-3′	50.5	50.5	53.0
ON4	5′-CCCCTT**Y**TCTTTTTT-3′	46.5	46.0	49.5
ON6	5′-CCCCTTTC**W**TTTTTT-3′	44.5	–[d]	–[d]
ON7	5′-CCCCTTTC**X**TTTTTT-3′	51.0	50.5	51.0
ON8	5′-CCCCTTTC**Y**TTTTTT-3′	46.0	46.0	49.0
ON10	5′-CCCCTTTCT**X**TTTTT-3′	51.0	51.0	53.0
ON11	5′-CCCCTTTCT**Y**TTTTT-3′	47.5	47.5	49.5
ON12	5′-CCCCTT**W**TCTWTTTTT-3′	41.0[c]	38.0[c]	–[d]
ON13	5′-CCCCTT**X**TCT**X**TTTTT-3′	49.0	50.5	49.5
ON14	5′-CCCCTT**Y**TCT**Y**TTTTT-3′	38.5	38.5	42.5
ON15	5′-**W**CCCCTTTCTTTTTT-3′	53.0[c]	52.0[c]	–[d]
ON16	5′-**X**CCCCTTTCTTTTTT-3′	56.5	56.5	59.0
ON17	5′-CCCCTTTCTTTTTT**X**-3′	54.0	54.0	55.5

[a] C = 1.0 μM of each oligonucleotide in 20 mM sodium cacodylate, 100 mM NaCl, 10 mM $MgCl_2$, pH 6.0 and 7.2.
[b] C = 1.0 μM of each oligonucleotide in 140 mM NaCl, 10 mM sodium phosphate buffer, 1 mM EDTA, pH 7.0.
[c] Data taken from Ref. 28a.
[d] Not reported in Ref. 28a.

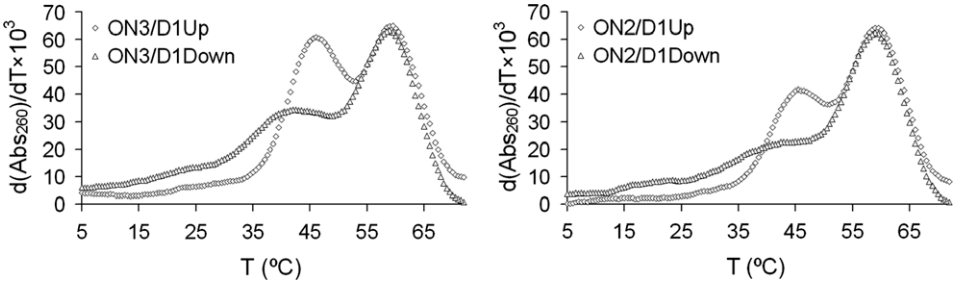

Figure 2. First derivatives plots of triplex melting (up and down) for **ON3** and **ON2** incorporating monomer **X** and **W**, respectively, recorded at 260 nm versus increasing temperature (1 °C/min) in 20 mM sodium cacodylate, 100 mM NaCl, 10 mM $MgCl_2$, pH 6.0.

insertions of **X** is due to intercalation and not an ionic interaction even at low pH. It was thought an advantage to replace the benzene ring in the intercalator **X** with the larger naphthalene ring to obtain the intercalator **Y** which was believed to give better stacking with the base pairs of the TFO. Such an effect has previously been reported for alternate strand triplexes.[37] However, considerably lower triplex meltings (6–15 °C at pH 6.0 and 7.2) were observed for the **Y** containing oligos **ON4**, **ON8**, and **ON11** than for the **X** containing oligos **ON3**, **ON7**, and **ON10**, respectively. This is explained under molecular modeling by sterical hindrance to planarity when naphthalene is incorporated into the intercalator. Attaching the intercalator **X** at the 5′-end (**ON16)** gave better stabilization of Hoogsteen-type triplexes and duplexes than at the 3′-end (**ON17**).

The parallel triplexes with bulge insertion of the intercalators **W**, **X**, and **Y** in the middle of the TFO were studied for their sensitivity to Hoogsteen mismatches at pH 6.0 (Table 2). For mono insertions, **X** was slightly better than **W** to discriminate neighboring Hoogsteen mismatches in **ON3** (15–23.5 °C) compared to **ON2** (11–18.5 °C), respectively. For **X**, it is approximately the same range that is found for discrimination for a non-neighboring insertion (**ON10**). The worst case for discrimination was actually found when the study was extended to TFOs with double insertions of the intercalators **X** and **Y** separated by three nucleobases. Here, the triplex containing **ON13/D4** gave the smallest change in ΔT_m = –9.5 °C for replacement of a T/A base pair with a G/C base pair in the duplex part of the triplex. The discriminating power of a mono inserted intercalator should be compared with the work of Zhou et

al.[38] who was actually aiming at stabilizing triplex forming of mismatch. They inserted 2-methoxy-6-chloro-9-aminoacridine in the middle of the TFOs as a bulge insertion and the ΔT_m values were in the range of 10 °C which is a much lower discriminating power than the ones found for our intercalators.

If the ultimate goal is to use modified TFOs as antigene oligos to control diseases, it is also important to consider the effect of the modification if the oligo can make stable complexes with other targets, e.g. forming a parallel duplex by Hoogsteen bonding or normal antiparallel DNA/DNA or DNA/RNA duplexes. Here, the TFOs were targeted in a parallel duplex fashion to the oligo **ON18**. As it can be seen from Table 1 considerable stabilizations (12.5–15.5 °C at pH 6.0) are achieved for the intercalator **X** for mono insertions when compared with the wild-type parallel duplex. This is slightly lower than the stabilizations (15.5–20.5 °C at pH 6.0) found for the corresponding triplexes. Besides it is important to note that the triplex melting is 9–17 °C higher than the corresponding parallel duplex melting.

The thermal stability studies of antiparallel Hoogsteen-type DNA/DNA duplexes were observed at pH 6.0, pH 7.2, and the corresponding DNA/RNA duplex was performed at pH 7.0 (Table 3). As shown for **ON2**, **ON6**, and **ON12**, destabilization has been described for oligos including the intercalator **W** in the middle of the oligo toward **ON19** in antiparallel Watson–Crick-type DNA/DNA duplexes, when compared with the wild-type duplex.[28a] Considering the similarity of **W** and **X** when used as conjugated bulge intercalators in triplex studies, it was surprising to find that the melting temperatures of both DNA/DNA and DNA/RNA duplexes with bulging **X** showed nearly identical melting temperatures to the corresponding wild-type duplexes (**ON3**, **ON7**, and **ON10**). This holds even for double insertion of **X** (**ON13**). When the intercalators **W** and **X** were placed at the 5′-end in **ON15**, **ON16**, respectively, or at the 3′-end in **ON17**, the stabilization effect was in the range ΔT_m = 3.5–7.0 °C for both DNA and RNA targeting. This is ascribed to stacking of the aromatic system on the adjacent nucleobases, which is known as the lid-effect.[39,40]

4. Fluorescence properties

The fluorescence measurements were performed for the single strand TFO (**ON3**) which was found effective to form triplexes and to discriminate Hoogsteen mismatches. The insertion of the intercalator **X** into oligonucleotides resulted in a characteristic monomeric fluorescence spectrum, with maxima at 400 nm upon excitation at 373 nm (Fig. 3). In all cases, a 4 nm shift of monomeric fluorescence was detected upon formation of triplexes or duplexes except in two cases **ON3/D3**, **ON3/D4**. The spectra were recorded from 340 to 600 nm at 10 °C in the same buffer solutions use for T_m studies using a 1.0 μM concentration of each strand of the unmodified duplex and modified TFO for the duplex and triplex measurements. Excitation and emission slits were set to 4 and 0.0 nm, respectively, the 0.0 nm slit not being totally dark. The fluorescence spectra of the TFO **ON3** toward **D1**, **D2**, **D3**, and **D4** were recorded at pH 6.0 and they are shown in Figure 3A. The fluorescence intensity increased of the fully matched triplex **ON3/D1** compared to the single-stranded **ON3**. However, the emission intensity of the triplex Hoogsteen mismatched **ON3/D2** decreased slightly because of an inverted A/T base pair in the duplex next to the intercalator compared to the matching triplex, On the contrary, when a Hoogsteen mismatch was due to a C/G base pair near the insertion of the intercalating **X** (**ON3/D3**, **ON3/D4**), the fluorescence intensity was even lower than the one of the single strand TFO. The fluorescence spectra of the oligo **ON3** toward **ON18**, **ON19** in parallel and antiparallel duplexes, respectively, are shown in Figure 3B. The emission intensity of the antiparallel duplex **ON3/ON19** is comparable to the one of the single strand **ON3** whereas the parallel duplex **ON3/ON18** showed increased fluorescence intensity.

5. Molecular modeling

The novel monomers **X** and **Y**s ability to stabilize the triplex via intercalation were studied using representative low-energy structures generated with the AMBER* force field in MacroModel 9.1. Molecular modeling was performed on truncated triplexes with the intercalator incorporated into the middle of the triplex. As it can be seen from Figure 4A–B, the position of the intercalators, **X** and **Y**, are similar and in both cases are the phenanthroimidazole moiety positioned in the Watson–Crick duplex thereby adding to the triplex stability via π–π-interaction. In addition, the phenyl- or naphthalene-moiety is positioned between nucleobases of the TFO, adding to the stability as well as ensuring equal amount of unwinding at the site of intercalation. In the case of intercalator **X**, the phenyl-moiety is only slightly twisted in comparison to the naphthalene-moiety of intercalator **Y** which is forced out of plane by sterical interaction between protons on the naphthalene-moiety and on the imidazole-moiety. The large extent of twisting between the two aromatic moieties of **Y** forces the nucleobases of the TFO to twist out of plane compared to **X**, thereby weakening the stacking interactions. This conclusion supports the thermal stability measurements which showed a decrease in triplex stability using intercalator **Y** in comparison with intercalator **X**, clearly demonstrating the importance of optimal π–π-stacking interactions. Twisting the naphthalene-moiety of intercalator **Y** around the single bond resulted in conformations with almost identical intercalating properties in the triplex and no optimal conformation could be assigned. In addition, protonation of the imidazole ring resulted in almost identical intercalating properties of the intercalator, but the protonated imidazole provided an alternative structure to the intercalating

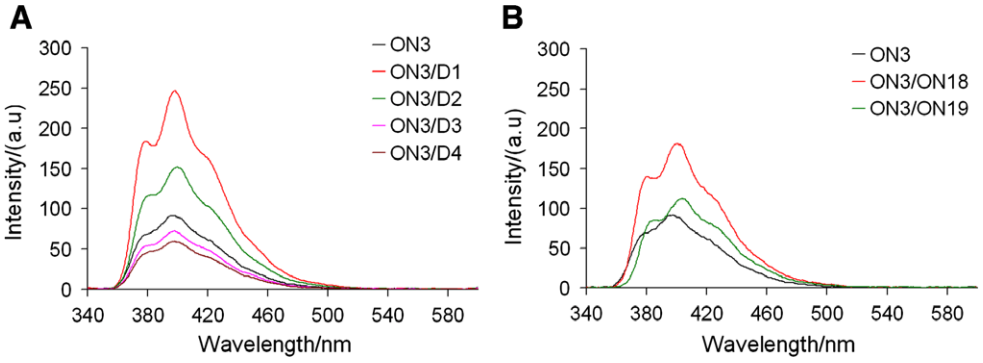

Figure 3. Fluorescence emission spectra of **ON3** incorporating monomer **X** upon excitation at 373 nm and pH 6.0. (A) **ON3** forming parallel triplex and mismatched triplexes. (B) **ON3** forming parallel duplex and antiparallel duplex.

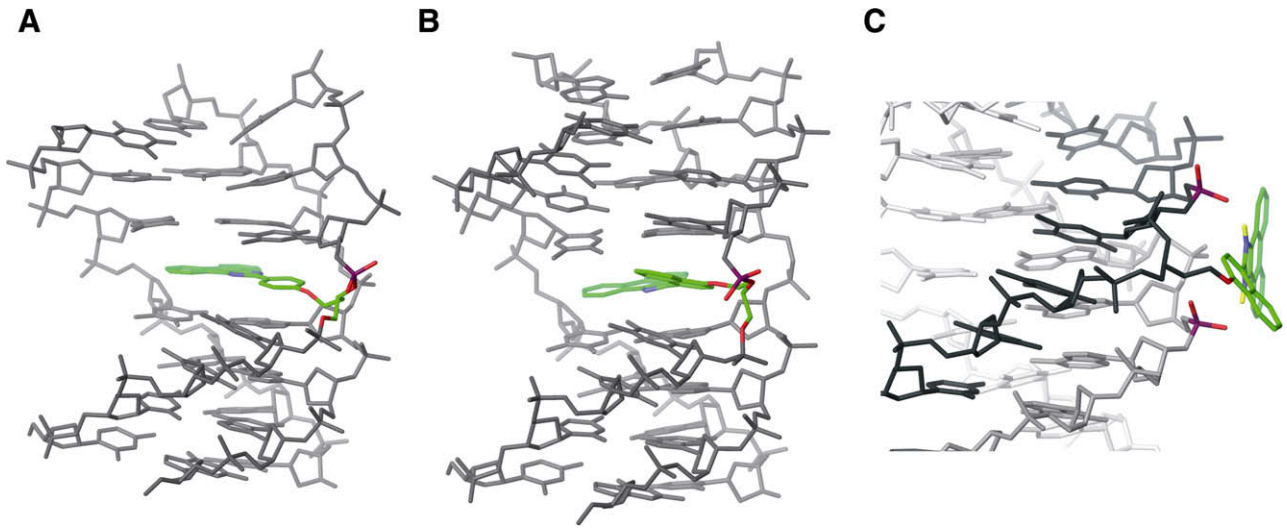

Figure 4. Representative low-energy structures triplexes intercalated by **X** (A) and **Y** (B), and the ionic interactions and hydrogen bondings between protonated **Y** and two phosphate groups (C).

structure. It was found that the protonated nitrogens of the imidazole ring positioned in the groove formed between the TFO and purine target were capable of forming ionic interactions and hydrogen bondings across the groove to two phosphate groups in each their backbone (Fig. 4C). This interaction could result in a stabilizing effect at low pH which not resulted from intercalation. Therefore, to investigate this possibility for an alternative stabilizing interaction, we synthesized the intercalator **Z**, which lacked the phenanthrene moiety and thereby should be unable to intercalate the triplex. The mode of triplex stabilization could be determined by experimentally comparing thermal stability of **Y** and **Z** at low pH, and the structure in Figure 4C was in that way ruled out.

6. Conclusion

Here, we have described the synthesis of two intercalating nucleic acid monomers **X** and **Y**, and their incorporation into oligonucleotides giving in good yield using normal oligonucleotide synthesis procedures. Melting studies showed that the two intercalators have extraordinary high thermal stability of Hoogsteen-type triplexes and duplexes with a high discrimination of mismatch strands. DNA-strands containing intercalator **X** show higher thermal triplex stability than DNA-strands containing intercalator **Y**. Interestingly, the intercalator **X** (**ON7**) slightly increased the triplex stability when compared to the intercalator **W** (TINA). In our research, the linker was the same atom number of the previous studies (TINA) but differs so that the oxygen atom was attached directly to the phenyl or naphthyl rings, respectively. The mode of intercalation was confirmed by the synthesis of intercalator **Z** which gave less stable parallel triplexes, when inserted as a bulge which means that the imidazol ring is too small to be an effective intercalator. In addition, an alternative ionic interaction across the groove formed between the TFO and purine target between protonated imidazol ring and negative by charge backbones was ruled out based on T_m determination at low pH.

7. Experimental

7.1. General

NMR spectra were recorded on a Varian Gemini 2000 spectrometer at 300 MHz for ^{1}H, 75 MHz for ^{13}C, and 121.5 MHz for ^{31}P with TMS as an internal standard for ^{1}H NMR, deuterated solvents $CDCl_3$ (δ 77.00 ppm), DMSO-d_6 (δ 39.44 ppm) for ^{13}C NMR, and 85% H_3PO_4 as an external standard for ^{31}P NMR. MALDI mass spectra of the synthesized compounds were recorded on a Fourier Transform Ion Cyclotron Resonance Mass Spectrometer (IonSpec, Irvine, CA). For accurate ion mass determinations, the (MH^+) or (MNa^+) ion was peak matched using ions derived from the 2,5-dihydroxybenzoic acid matrix. Electrospray ionization mass spectra (ESI-MS) were performed on a 4.7 T HiResESI Uitima (FT) mass spectrometer. Both spectrometers are controlled by the OMEGA Data System. Melting points were determined on a Büchi melting point apparatus. Silica gel (0.040–0.063 mm) used for column chromatography and analytical silica gel TLC plates 60 F_{254} were purchased from Merck. Solvents used for column chromatography were distilled prior to use, while reagents were used as purchased. Petroleum ether (PE): bp 60–80 °C.

7.1.1. General procedure for preparation of 3 in a Mitsunobu reaction

An ice-cooled solution of diethylazodicarboxylate (DEAD, 2.5 ml, 16 mmol) in dry THF (155 ml) was treated with (*S*)-2-(2,2-dimethyl-1,3-dioxolan-4-yl)ethanol (**1**) (1.9 ml, 13 mmol) for 25 min, and then 4-hydroxybenzaldehyde (**2a**) (2.1 g, 17 mmol) or 4-hydroxy-1-naphthaldehyde (**2b**) (3.0 g, 17 mmol) and triphenylphosphine (4.2 g, 16 mmol) were added to the mixture. The mixture was stirred in an ice-water bath for 30 min, and then allowed to warm to room temperature overnight. The mixture was quenched with aqueous ammonia (105 ml) and extracted with AcOEt. The organic layer was washed with water, dried over $MgSO_4$, and concentrated under reduced pressure to leave an oil which was purified by silica gel column chromatography [petroleum ether/diethyl ether (1:1, v/v)] to afford the pure products (**3a,b**).

7.1.2. (*S*)-4-(2-(2,2-Dimethyl-1,3-dioxolan-4-yl)ethoxy)benzaldehyde (3a)

Yield: 3.5 g (81%) as an oil; R_f 0.30 (50% petroleum ether/diethyl ether). ^{1}H NMR ($CDCl_3$): δ 1.38 (s, 3H, CH_3), 1.44 (s, 3H, CH_3), 2.08 (m, 2H, CH_2CH_2O), 3.67 (m, 1H, CH*H*), 4.12–4.22 (m, 3H, C*H*H and CH_2CH_2O), 4.32 (m, 1H, C*H*), 7.01 (d, 2H, J = 8.7 Hz, aryl), 7.84 (d, 2H, J = 8.7 Hz, aryl), 9.88 (s, 1H, C*H*O). ^{13}C NMR ($CDCl_3$): δ 25.6 (CH_3), 26.9 (CH_3), 33.3 (CH_2CH_2O), 65.1 (CH_2CH_2O), 69.4 ($CH_2OC(CH_3)_2$), 73.0 (CH_2CHCH_2), 108.9 ($C(CH_3)_2$), 114.6, 130.0,

131.9, 163.8 (aryl), 190.7 (CHO). HRMS (ESI) *m*/*z* Calcd for $C_{14}H_{18}O_4Na^+$ (MNa^+) 273.1097. Found: 273.1101.

7.1.3. (*S*)-4-(2-(2,2-Dimethyl-1,3-dioxolan-4-yl)ethoxy)-1-naphthaldehyde (3b)

Yield 4.8 g (92%) as an oil; R_f 0.31 (50% petroleum ether/diethyl ether). ^{1}H NMR ($CDCl_3$): δ 1.39 (s, 3H, CH_3), 1.44 (s, 3H, CH_3), 2.23 (m, 2H, CH_2CH$_2$O), 3.74 (dd, 1H, *J* = 7.2, 8.1 Hz, CH*H*), 4.21 (m, 1H,C*H*), 4.39 (m, 3H, CH$_2$CH_2O, C*H*H), 6.93 (d, 1H, *J* = 8.1 Hz, aryl), 7.57–7.60 (m, 1H, aryl), 7.68–7.71 (m, 1H, aryl), 7.90 (d, 1H, *J* = 8.1 Hz, aryl), 8.31 (d, 1H, *J* = 9.0 Hz, aryl), 9.31(d, 1H, *J* = 9.0 Hz, aryl), 10.20 (s, 1H, CHO). ^{13}C NMR ($CDCl_3$): δ 25.7 (CH_3), 27.0 (CH_3), 33.4 (CH_2CH_2O), 65.5 (CH_2CH_2O), 69.5 ($CH_2OC(CH_3)_2$), 73.2 (CH_2CHCH_2), 103.6 (aryl), 109.1 ($C(CH_3)_2$), 122.2, 124.9, 125.0, 125.4, 126.7, 129.5, 131.9, 139.6, 159.9 (aryl), 192.2 (CHO). HRMS (ESI) *m*/*z* Calcd for $C_{18}H_{20}O_4Na^+$ (MNa^+) 323.1254. Found: 323.1264.

7.1.4. General procedure for preparation of the phenanthroimidazol compounds 6

Phenanthrene-9,10-dione (1 equiv) and ammonium acetate (16.5 equiv) were dissolved in hot glacial acetic acid (10 ml). While the mixture was stirred, a solution of (*S*)-4-(2-(2,2-dimethyl-1,3-dioxolan-4-yl)ethoxy)benzaldehyde (**3a**, 2.0 g, 8.0 mmol) or (*S*)-4-(2-(2,2-dimethyl-1,3-dioxolan-4-yl)ethoxy)-1-naphthaldehyde (**3b**, 1.0 g, 3.3 mmol) in 10 ml of glacial acetic acid was added dropwise. The mixture was heated at 90 °C for 3 h and was then poured in to water (200 ml). The mixture was neutralized with aqueous ammonia to pH 7 and then cooled to room temperature. The precipitate was filtered off and washed with large portions of H_2O. The residue was purified by silica gel column chromatography [MeOH/CH_2Cl_2 (1:1, v/v)] afforded **5** and **6a**. Compound **6b** was obtained directly from the precipitate without using chromatography. Recrystallization from toluene and one drop of NEt_3.

7.1.5. (*S*)-2-(4-(2-(2,2-Dimethyl-1,3-dioxolan-4-yl)ethoxy)phenyl)-1*H*-phenanthro[9,10-*d*] imidazole (5)

Yield 0.30 g (8.5%) as solids; R_f 0.55 (50% MeOH/CH_2Cl_2); mp 196–198 °C. ^{1}H NMR ($CDCl_3$): δ 1.35 (s, 3H, CH_3), 1.41 (s, 3H, CH_3), 1.91 (m, 2H, CH_2CH$_2$O), 3.55 (m, 1H, CH*H*), 3.82 (m, 2H, C*H*H, CH$_2$CH*H*O), 4.05 (m, 1H, CH$_2$C*H*HO), 4.18 (m, 1H, C*H*), 6.64 (d, 2H, *J* = 8.7 Hz, aryl), 7.54 (m, 4H, aryl), 7.89 (d, 2H, *J* = 8.7 Hz, aryl), 8.43 (br s, 2H, aryl), 8.67 (m, 2H, aryl). ^{13}C NMR ($CDCl_3$): δ 25.7 (CH_3), 26.9 (CH_3), 33.3 (CH_2CH_2O), 64.5 (CH_2CH_2O), 69.5 ($CH_2OC(CH_3)_2$), 73.3 (CH_2CHCH_2), 108.8 ($C(CH_3)_2$), 114.5, 121.7, 122.7–128.2 (aryl), 149.35 (C=N, aryl), 159.7 (aryl). HRMS (MALDI) *m*/*z* Calcd for $C_{28}H_{27}N_2O_3^+$ (MH^+) 439.2016. Found: 439.2002.

7.1.6. (*S*)-4-(4-(1*H*-Phenanthro[9,10-*d*]imidazol-2-yl)phenoxy)-butane-1,2-diol (6a)

Yield 2.3 g (72%) as solids; R_f 0.10 (50% MeOH/CH_2Cl_2); mp 263–265 °C. ^{1}H NMR (DMSO-d_6): δ 1.77 (m, 1H, CH*H*CH$_2$O), 2.04 (m, 1H, C*H*HCH$_2$O), 3.42 (m, 2H, CH*H*OH and C*H*OH), 3.76 (m, 1H, C*H*HOH), 4.23 (m, 2H,CH$_2$CH_2O), 4.69, 4.76 (2s, 2H, 2× OH), 7.20 (d, 2H, *J* = 8.7 Hz, aryl), 7.63 (m, 2H, aryl), 7.75 (m, 2H, aryl), 8.30 (d, 2H, *J* = 8.7 Hz, aryl), 8.61 (d, 2H, *J* = 8.1 Hz, aryl), 8.83 (d, 2H, *J* = 8.1 Hz, aryl), 13.32 (br s, 1H, NH). ^{13}C NMR (DMSO-d_6): δ 33.1 (CH_2CH_2O), 64.8 (CH_2CH_2O), 66.0 ($CHCH_2OH$), 68.1 ($CHCH_2OH$), 114.8, 121.9, 122.8–127.7 (aryl), 149.4 (C=N, aryl), 159.7 (aryl). HRMS (MALDI) *m*/*z* Calcd for $C_{25}H_{23}N_2O_3^+$ (MH^+) 399.1703. Found: 399.1689.

7.1.7. (*S*)-4-(4-(1*H*-Phenanthro[9,10-*d*]imidazol-2-yl)naphalen-1-yloxy)butane-1,2-diol (6b)

Yield 1.2 g (80%) as solids; mp 165–167 °C. ^{1}H NMR (DMSO-d_6): δ 2.05 (m, 2H, CH_2CH$_2$O), 3.61 (m, 1H, C*H*OH), 3.85 (m, 1H, CH*H*OH), 4.06 (m, 1H, C*H*HOH), 4.41 (m, 2H, CH_2O), 4.73, 5.16 (2 br s, 2H, 2× OH), 7.23 (d, 1H, *J* = 7.8 Hz, aryl), 7.61–7.78 (m, 7H, aryl), 8.09 (d, 1H, *J* = 8.1 Hz, aryl), 8.36 (d, 1H, *J* = 7.8 Hz, aryl), 8.61 (m, 1H, aryl), 8.88 (m, 2H, aryl), 9.24 (d, 1H, *J* = 8.1 Hz, aryl), 13.49 (br s, 1H, NH). ^{13}C NMR (DMSO-d_6): δ 33.1 (CH_2CH_2O), 65.2 (CH_2CH_2O), 66.1 ($CHCH_2OH$), 68.2 ($CHCH_2OH$), 104.6, 120.0, 121.9, 122.0–131.7 (aryl), 149.6 (C=N, aryl), 155.3 (aryl). HRMS (ESI) *m*/*z* Calcd for $C_{29}H_{25}N_2O_3^+$ (MH^+) 449.1860. Found: 449.1864.

7.1.8. General procedure for preparation of 7 by DMT-protection

(*S*)-4-(4-(1*H*-Phenanthro[9,10-d]imidazol-2-yl)phenoxy)butane-1,2-diol (**6a**, 1.0 g, 2.5 mmol) or (*S*)-4-(4-(1*H*-phenanthro[9,10-d]imidazol-2-yl)naphalen-1-yloxy)butane-1,2-diol (**6b**, 0.50 g, 1.11 mmol) was dissolved in anhydrous pyridine (20 ml). 4,4′-Dimethoxytrityl chloride (1.2 equiv) was added under a nitrogen atmosphere, and the reaction mixture was stirred at room temperature for 24 h. The reaction was quenched by addition of MeOH (2 ml) followed by addition of EtOAc (75 ml), and extracted with saturated aqueous $NaHCO_3$ (2× 20 ml). The H_2O phase was extracted with EtOAc (2× 10 ml), and the combined organic phases were dried (Na_2SO_4), filtered, and evaporated under diminished pressure. The residue was coevaporated twice with toluene/EtOH 15 ml, (1:1, v/v). The residue was purified by silica gel column chromatography [NEt_3 (0.5%, v/v)/EtOAc (40–50%)/cyclohexane] to afford the DMT-protected diols **7a,b**.

7.1.9. (*S*)-4-(4-(1*H*-Phenanthro[9,10-*d*]imidazol-2-yl)phenoxy)-1-(bis(4-methoxyphenyl) (phenyl)methoxy)butan-2-ol (7a)

Yield 1.4 g (79%) as a foam; R_f 0.43. ^{1}H NMR ($CDCl_3$): δ 1.85 (m, 2H, CH_2CH$_2$O), 3.18 (m, 2H, CH_2ODMT), 3.72 (s, 6H, 2× OCH_3), 3.89 (m, 2H, CH$_2$CH_2O), 4.04 (m, 1H, C*H*OH), 6.66 (d, 2H, *J* = 8.4 Hz, aryl), 6.77 (d, 4H, *J* = 8.7 Hz, DMT), 7.17–7.30 (m, 9H, aryl), 7.40 (d, 2H, *J* = 7.2 Hz, aryl), 7.55 (m, 4H, aryl), 7.88 (d, 2H, *J* = 8.4 Hz, aryl), 8.44 (br s, 1H, NH), 8.69 (m, 2H, aryl). ^{13}C NMR ($CDCl_3$): δ 33.0 (CH_2CH_2O), 55.2 (2× OCH_3), 64.7 (CH_2CH_2O), 67.4 (CHOH), 68.4 (CH_2ODMT), 86.2 ($OCPh_3$), 113.1, 114.7, 122.7–130.0, 135.9, 144.8, 149.6, 158.5, 159.7 (aryl). HRMS (ESI) *m*/*z* Calcd for $C_{46}H_{41}N_2O_5^+$ (MH^+) 701.3010. Found: 701.3044.

7.1.10. (*S*)-4-(4-(1*H*-Phenanthro[9,10-*d*]imidazol-2-yl)naphthalen-1-yloxy)-1-(bis(4-methoxy phenyl)(phenyl)methoxy)butan-2-ol (7b)

Yield 0.47 g (56%) as a foam; R_f 0.34. ^{1}H NMR ($CDCl_3$): δ 1.90 (m, 2H, CH_2CH$_2$O), 3.02 (br s, 1H, OH), 3.18 (m, 2H, CH_2ODMT), 3.75 (s, 6H, 2× OCH_3), 3.93 (m, 2H, CH_2 CH_2O), 4.07 (m, 1H, C*H*OH), 6.33 (m, 1H, aryl), 7.76 (d, 4H, *J* = 8.4 Hz, DMT), 7.18−7.55 (m, 18H, aryl), 8.04 (d, 1H, *J* = 7.5 Hz, aryl), 8.55 (d, 1H, *J* = 7.5 Hz, aryl), 8.69 (m, 2H, aryl), 11.31 (br s, 1H, NH). ^{13}C NMR ($CDCl_3$): δ 33.1 (CH_2CH_2O), 55.2, 55.2 (2× OCH_3), 64.8 (CH_2 CH_2O), 67.5 (CHOH), 68.5 (CH_2ODMT), 86.2 ($OCPh_3$), 103.7, 113.1, 120.2, 122.0, 125.1–130.0, 132.1, 135.9, 144.8 (aryl), 149.5 (C=N, aryl), 155.5, 158.4 (aryl). HRMS (ESI) *m*/*z* Calcd for $C_{50}H_{42}N_2O_5Na^+$ (MNa^+) 773.2987. Found: 773.3003.

7.1.11. General procedure for preparation of phosphoramidite (8)

DMT-protected compound **7a** (0.4 g, 0.57 mmol) or **7b** (0.1 g, 0.17 mmol) was dissolved under an argon atmosphere in anhydrous CH_2Cl_2 (10–15 ml). *N*,*N*′-Diisopropylammonium tetrazolide (1.5 equiv) was added, followed by dropwise addition of 2-cyanoethyl *N*,*N*,*N*′,N′-tetraisopropylphosphordiamidite (3 equiv) under external cooling with an ice-water bath. The reaction mixture was stirred at room temperature overnight. After 24 h, analytical TLC showed no more starting material and the reaction was

quenched with H_2O (10–20 ml). The layers were separated and the organic phase was washed with H_2O (10–20 ml), the combined water layers were washed with CH_2Cl_2 (25 ml), the organic phase was dried (Na_2SO_4) and filtered, and the solvents were evaporated in vacuo. The residue was purified by silica gel column chromatography [NEt_3 (0.5%, v/v)/EtOAc (40–50%)/cyclohexane] to afford the final products **8a,b** as a foam, which were used in DNA synthesis after drying under diminished pressure.

7.1.12. (*S*)-4-(4-(1*H*-Phenanthro[9,10-*d*]imidazol-2-yl)phenoxy)-1-(bis(4-methoxyphenyl)(phenyl)-methoxy)butan-2-yl 2-cyanoethyl diisopropylphosphoramidite (8a)

Yield 0.44 g (86%) as a foam; R_f 0.68. ^{13}C NMR ($CDCl_3$): δ 20.1 (CH_2CN), 24.4, 24.5, 24.6, 24.7 (2× $CH(CH_3)_2$), 33.0 (CH_2CH_2O), 43.1, 43.2 (2× $C(CH_3)_2$), 55.2 (2× OCH_3), 57.8 (OCH_2CH_2CN), 64.1 (CH_2CH_2O), 66.4 (CHOP $[NPr_2]_2$), 69.4 (CH_2ODMT), 86.0 ($OCPh_3$), 113.0, 114.9, 122.5–130.1, 136.1, 136.2, 144.9, 149.8, 158.4, 158.4, 160.0 (aryl). ^{31}P NMR ($CDCl_3$): δ 149.98, 150.05 in a 5:4 ratio. HRMS (ESI) *m*/*z* Calcd for $C_{55}H_{57}N_4O_6PNa^+$ (MNa^+) 923.3909. Found: 923.3913.

7.1.13. (*S*)-4-(4-(1*H*-Phenanthro[9,10-*d*]imidazol-2-yl)naphthalen-1-yloxy)-1-(bis(4-methoxy phenyl)(phenyl)methoxy)butan-2-yl 2-cyanoethyl diisopropylphosphoramidite (8b)

Yield 0.11 g (81%) as a foam; R_f 0.64. ^{13}C NMR ($CDCl_3$): δ 20.08 (CH_2CN), 24.4, 24.5, 24.6, 24.7 (2× $CH(CH_3)_2$), 33.0 (CH_2CH_2O), 43.1, 43.3 (2× $CH(CH_3)_2$), 55.2 (2× OCH_3), 57.9 (OCH_2CH_2CN), 64.2 (CH_2CH_2O), 66.4 (CHOP$[NPr_2]_2$), 70.8 (CH_2ODMT), 86.1 ($OCPh_3$), 104.0, 113.1, 117.7, 120.6–132.5, 136.1, 136.2, 145.0, 149.5, 155.8, 158.4 (aryl). ^{31}P NMR ($CDCl_3$): δ 149.98, 150.48 in a 2:1 ratio. HRMS (ESI) *m*/*z* Calcd for $C_{59}H_{59}N_4O_6PNa^+$ (MNa^+) 973.4065. Found: 973.4021.

7.1.14. (*S*)-4-(3,4-Dihydroxybutoxy)-1-naphthaldehyde (9)

Compound **3b** (0.85 g, 2.83 mmol) was stirred in 80% acetic acid (25 ml) for 24 h at room temperature. The solvent was removed in vacuo, and the residue was coevaporated twice with toluene/EtOH (30 ml, 5:1, v/v). The residue was dried in vacuo to afford 4-(3,4-dihydroxybutoxy)-1-naphthaldehyde **9**. Yield 0.74 g (100%) as an oil which was used in the next step without further purification. ^1H NMR (DMSO-d_6): δ 1.83 (m, 1H, C*H*HCH$_2$O), 2.30 (m, 1H, CH*H*CH$_2$O), 3.42 (m, 2H, CH$_2$C*H*OH , CH*H*OH), 3.80 (m, 1H, C*H*HOH), 4.42 (m, 2H, CH$_2$C*H*$_2$O), 4.63, 4.73 (s, 2H, 2× OH), 7.22 (m, 1H, aryl), 7.64 (m, 1H, aryl), 7.75 (m, 1H, aryl), 8.14 (d, 1H, *J* = 8.1 Hz, aryl), 8.31 (d, 1H, *J* = 7.8 Hz, aryl), 9.23 (d, 1H, *J* = 8.4 Hz, aryl), 10.18 (s, 1H, CHO). ^{13}C NMR (DMSO-d_6): δ 32.8 (CH_2CH_2O), 65.7 (CH_2CH_2O), 65.9 (CH_2OH), 68.0 (CHOH), 104.6, 122.1–131.1, 140.4, 159.6 (aryl), 192.7 (CHO). HRMS (ESI) *m*/*z* Calcd for $C_{15}H_{16}O_4Na^+$ (MNa^+) 283.0941. Found: 283.0948.

7.1.15. (*S*)-4-(4-(1*H*-Imidazol-2-yl)naphthalen-1-yloxy)butan-1,2-diol (10)

To a solution of (*S*)-4-(3,4-dihydroxybutoxy)-1-naphthaldehyde (**9**, 0.10 g, 0.38 mmol) in EtOH (0.54 ml) was added about dry MeCN (3 ml) to give a clear solution. Forty percent of glyoxal in H_2O (0.10 ml, 1.93 mmol) and 20 M ammonium hydroxide (0.13 ml) was added at 0 °C. The mixture was stirred for 30 min at 0 °C and then at room temperature overnight. The mixture was concentrated in vacuo and the residue was purified by silica gel column chromatography [EtOAc/cyclohexane/NEt_3 (90:8:2, v/v/v)] to give compound **10**. Yield 0.05 g (44%) as an oil; R_f 0.11. ^1H NMR (DMSO-d_6): δ 2.04 (m, 2H, CH_2CH$_2$O), 3.42 (m, 2H, C*H*OH and CH*H*OH), 3.80 (m, 1H, CH*H*OH), 4.36 (m, 2H, CH$_2$CH_2O), 4.69, 4.71 (2s, 2H, 2× OH), 6.70–8.01 (m, 6H, aryl), 8.27 (d, 1H, *J* = 8.7 Hz, aryl), 9.01 (d, 1H, *J* = 8.7 Hz, aryl), 12.38 (br s, 1H, NH). ^{13}C NMR (DMSO-d_6): δ 33.1 (CH_2CH_2O), 65.0 (CH_2CH_2O), 66.0 (CH_2OH), 68.1 (CHOH), 104.2, 120.4, 121.5, 125.4, 126.8, 128.1, 129.8, 131.2, 134.8, 145.4, 154.3 (aryl). HRMS (MALDI) *m*/*z* Calcd for $C_{17}H_{18}N_2O_3Na^+$ (MNa^+) 321.1210. Found: 321.1217.

7.1.16. (*S*)-4-(4-(Bis(4-methoxyphenyl)(phenyl)methoxy)-3-hydroxybutoxy)-1-naphthaldehyde (11)

Compound **9** (0.50 g, 1.92 mmol) was dissolved in dry pyridine (20 ml) and 4,4′-dimethoxytrityl chloride (DMT-Cl) (0.78 g, 2.30 mmol) was added under a nitrogen atmosphere. The reaction mixture was stirred for 24 h at room temperature. The solvent was evaporated off under reduced pressure, and the residue was purified by silica gel column chromatography [NEt_3 (0.5%, v/v)/EtOAc (30–50%)/cyclohexane] affording compound **11**. Yield 0.65 g (60%) as a foam; R_f 0.21. ^1H NMR ($CDCl_3$): δ 2.08 (m, 2H, CH_2CH$_2$O), 2.49 (s, 1H, OH), 3.21, 3.32 (2× m, 2H, CH_2ODMT), 3.76 (s, 6H, 2× OCH_3), 4.13 (m, 1H, C*H*OH), 4.34 (m, 2H, CH$_2$CH_2O), 6.80 (d, 4H, *J* = 9.0 Hz, DMT), 6.86 (d, 1H, *J* = 8.1 Hz, aryl), 7.29 (m, 8H, aryl), 7.43 (d, 1H, *J* = 6.9 Hz, aryl), 7.56 (m, 1H, aryl), 7.72 (m, 1H, aryl), 7.89 (d, 1H, *J* = 8.1 Hz, aryl), 8.22 (d, 1H, *J* = 8.4 Hz, aryl), 9.30 (d, 1H, *J* = 8.4 Hz, aryl), 10.19 (s, 1H, CHO). ^{13}C NMR ($CDCl_3$): δ 32.9 (CH_2CH_2O), 55.2 (2× OCH_3), 65.3 (CH_2CH_2O), 67.4 (*C*HOH), 68.2 (CH_2ODMT), 86.3 ($OCPh_3$), 103.7, 113.2, 122.3–130.0, 131.9, 135.8, 139.7, 144.7, 158.5, 160.0 (aryl), 192.3 (CHO). HRMS (ESI) *m*/*z* Calcd for $C_{36}H_{34}O_6Na^+$ (MNa^+) 585.2248. Found: 585.2253.

7.1.17. (*S*)-4-(4-(1*H*-Imidazol-2-yl)naphthalen-1-yloxy)-1-(bis(4-methoxyphenyl)(phenyl)-methoxy)butan-2-ol (12)

To a solution of (*S*)-4-(4-(bis(4-methoxyphenyl)(phenyl)methoxy)-3-hydroxybutoxy)-1-naphthaldehyde (**11**) (0.44 g, 0.79 mmol) in EtOH (1.1 ml) was added dry MeCN (5 ml) to give a clear solution. Forty percent of glyoxal in H_2O (0.18 ml, 4.0 mmol) and 20 M ammonium hydroxide (0.27 ml) was added at 0 °C. The mixture was stirred for 30 min at 0 °C and then at room temperature under a nitrogen atmosphere overnight. The reaction mixture was concentrated in vacuo and the residue was purified by silica gel column chromatography [EtOAc/cyclohexane/NEt_3 (90:8:2, v/v/v)] affording compound **12**. Yield 0.15 g (32%) as a foam; R_f 0.50. ^1H NMR ($CDCl_3$): δ 1.94 (m, 2H, CH_2CH$_2$O), 3.19, 3.29 (2× m, 2H, CH_2ODMT), 3.74 (s, 6H, 2× OCH_3), 4.11 (m, 4H, CH$_2$CH_2O and C*H*OH), 6.55 (d, 1H, *J* = 8.1 Hz, aryl), 6.78 (d, 4H, *J* = 8.7 Hz, DMT), 7.08 (s, 2H, imidazole), 7.19–7.31 (m, 7H, aryl), 7.41 (m, 5H, aryl), 8.16 (d, 1H, *J* = 9.0 Hz, aryl), 8.44 (d, 1H, *J* = 8.1 Hz, aryl). ^{13}C NMR ($CDCl_3$): δ 33.1 (CH_2CH_2O), 55.2 (2× OCH_3), 64.8 (CH_2CH_2O), 67.5 (CHOH), 68.4 (CH_2ODMT), 86.2 ($OCPh_3$), 103.8, 113.1, 120.7, 122.1, 125.4–130.0, 132.0, 135.9, 136.0, 144.8, 146.4, 155.2, 158.4 (aryl). HRMS (ESI) *m*/*z* Calcd for $C_{38}H_{36}N_2O_5Na^+$ (MNa^+) 623.2517. Found: 623.2494.

7.1.18. (*S*)-4-(4-(1*H*-Imidazol-2-yl)naphthalen-1-yloxy)-1-(bis(4-methoxyphenyl)(phenyl)-methoxy)butan-2-yl 2-cyanoethyl diisopropylphosphoramidite (13)

Compound **12** (0.10 g, 0.17 mmol) was dissolved under an argon atmosphere in anhydrous CH_2Cl_2 (10 ml). *N*,*N*′-Diisopropyl ammonium tetrazolide (0.04 g, 0.25 mmol) was added, followed by dropwise addition of 2-cyanoethyl tetraisopropylphosphordiamidite (0.15 g, 0.45 mmol) under external cooling with an ice-water bath. The reaction mixture was stirred at room temperature under an argon atmosphere overnight. After 24 h, analytical TLC showed no more starting material. The solvent was evaporated under reduced pressure and the residue was purified by silica gel column chromatography [EtOAc/cyclohexane/NEt_3 (90:8:2, v/v/v)] affording compound **13**. Yield: 0.11 g (81%) as a foam; R_f 0.70. ^{13}C NMR ($CDCl_3$): δ 20.2 (CH_2CN), 24.4, 24.5, 24.6, 24.7 [2× $CH(CH_3)_2$], 33.2 (CH_2CH_2O), 43.0, 43.2 [2× $CH(CH_3)_2$], 55.2 (2× OCH_3), 57.7 (OCH_2CH_2CN), 64.3 (CH_2CH_2O), 66.5 (CHOP$[NPr_2]_2$), 71.0 (CH_2ODMT), 86.0 ($OCPh_3$), 104.0, 113.0, 121.0, 122.2, 125.4–

130.1, 132.2, 136.1, 136.2, 144.9, 146.5, 155.3, 158.4 (aryl). ^{31}P NMR ($CDCl_3$): δ 149.99, 150.09 in a 4:3 ratio. HRMS (ESI) *m*/*z* Calcd for $C_{47}H_{53}N_4O_6PNa^+$ (MNa^+) 823.3585. Found: 823.3581.

7.2. Oligonucleotide synthesis, purification, and melting temperature determination

DMT-on oligodeoxynucleotides were carried out at 0.2 μmol scales on 500 Å CPG supports with an *Expedite*™ Nucleic Acid Synthesis System Model 8909 from Applied Biosystems with 1*H*-tetrazole as an activator for coupling reaction. The appropriate amidite (**8a**,**b** and **13**) was dissolved in dry CH_2Cl_2 and inserted into the growing oligonucleotides chain using an extended coupling time (10 min). DMT-on oligonucleotides bound to CPG supports were treated with aqueous ammonia (32%, 1 ml) at room temperature and then at 55 °C overnight. Purification of 5′-*O*-DMT-on ONs was accomplished by reversed-phase semipreparative HPLC on a Waters Xterra MS C_{18} column with a Waters Delta Prep 4000 Preparative Chromatography System (Buffer A [0.05M triethylammonium acetate in H_2O (pH 7.4)] and Buffer B (75% MeCN in H_2O)). Flow 2.5 ml min^{-1}. Gradients: 2 min 100% A, linear gradient to 70% B in 38 min, linear gradient to 100% B in 3 min and then 100% A in 10 min). ODNs were DMT deprotected in 100 μL 80% acetic acid over 20 min. Afterwards, aqueous AcONa (1 M, 50 μL) was added and the ONs were precipitated from EtOH (96%). All modified ODNs were confirmed by MALDI-TOF analysis on a Voyager Elite Bio spectroscopy Research Station from PerSeptive Biosystems. ODN Found *m*/*z* (Calculated *m*/*z*): **ON2** 4589.3 (4589.2), **ON3** 4580.1 (4581.3), **ON4** 4627.3 (4631.3), **ON5** 4476.5 (4481.1), **ON7** 4579.1 (4581.3), **ON8** 4629.2 (4631.3), **ON9** 4479.5 (4481.1), **ON10** 4591.7 (4581.3), **ON11** 4627.6 (4631.3), **ON13** 5042.7 (5040.7), **ON14** 5138.2 (5140.8), **ON16** 4578.9 (4581.3), and **ON17** 4576.8 (4581.3). The purity of the final TFOs was found to be over 90%, checked by ion-exchange chromatography using LaChrom system from Merck Hitachi on Genpak-Fax column (Waters). Melting temperature measurments were performed on a Perkin-Elmer UV/vis spectrometer Lambda 35 fitted with a PTP-6 temperature programmer. The triplexes were formed by first mixing the two strands of the Watson–Crick duplex, each at a concentration of 1.0 μM, followed by addition of the third (TFO) strand at a concentration of 1.5 μM in a buffer consisting of sodium cacodylate (20 mM), NaCl (100 mM), and $MgCl_2$ (10 mM) at pH 6.0 or 7.2. Parallel and antiparallel duplexes were formed by mixing of complementary ONs, each at a concentration of 1.0 μM, in the cacodylate buffer described above. Antiparallel duplex was formed by mixing of complementary ONs, each at a concentration of 1.0 μM in sodium phosphate buffer (10 mM) containing NaCl (140 mM) and EDTA (1 mM) at pH 7.0. The solutions were heated to 80 °C for 5 min and cooled to 5 °C and were then kept at this temperature for 30 min. The melting temperature (T_m, °C) was determined as the maximum of the first derivative plots of the melting curves obtained by absorbance at 260 nm against increasing temperature (1.0 °C/min). If needed experiments were also done at 373 nm. All melting temperatures are within the uncertainly ±1.0 °C as determined by repetitive experiments.

7.3. Fluorescence measurements

The fluorescence measurements were measured on a Perkin-Elmer LS-55 luminescence spectrometer fitted with a julabo F25 temperature controller set at 10 °C in the buffer 20 mM sodium cacodylate, 100 mM NaCl, and 10 mM $MgCl_2$ at pH 6.0. The triplexes and duplexes were formed in the same way as for T_m measurements except that only 1.0 μM of TFOs were used in all cases. The excitation wave length was set to 373 nm. Excitation and emission slits were set to 4 nm and 0.0 nm, respectively. The 0.0 nm slit is not completely closed and allowed sufficient light to pass for the measurement.

7.4. Molecular modeling

Molecular modeling was performed with Macro Model v9.1 from Schrödinger. All calculations were conducted with AMBER* force field and the GB/SA water model. The dynamic simulations were preformed with stochastic dynamics, a SHAKE algorithm to constrain bonds to hydrogen, time step of 1.5 fs and simulation temperature of 300 K. Simulation for 0.5 ns with an equilibration time of 150 ps generated 250 structures, which all were minimized using the PRCG method with convergence threshold of 0.05 kJ/mol. The minimized structures were examined with Xcluster from Schrödinger, and representative low-energy structures were selected. The starting structures were generated with Insight II v97.2 from MSI, followed by incorporation of the modified nucleotide.

Acknowledgments

This work supported by the Sixth Framework Program Marie Curie Host Fellowships for Early Stage Research Training under contract number MEST-CT-2004-504018 and by the Nucleic Acid Center, which is funded by The Danish National Research Foundation for studies on nucleic acid chemical biology.

References and notes

1. Vasquez, K. M.; Wilson, J. M. *Trends Biochem. Sci.* **1998**, *23*, 4.
2. Maher, L. J. *Cancer Invest.* **1996**, *14*, 66.
3. Neidle, S. *Anti-Cancer Drug Des.* **1997**, *12*, 433.
4. Wang, G.; Levy, D. D.; Seidman, M. M.; Glazer, P. M. *Mol. Cell. Biol.* **1995**, *15*, 1759.
5. Majumdar, A.; Khorlin, A.; Dyatkina, N. B.; Lin, M. F.; Powell, J.; Fei, Z.; Khripine, Y.; Watanabe, K. A.; George, J.; Glazer, P. M.; Seidman, M. M. *Nat. Genet.* **1998**, *20*, 212.
6. Vasquez, K. M.; Naryanan, L.; Glazer, P. M. *Science* **2000**, *290*, 530.
7. Guntaka, R. V.; Varma, B. R.; Weber, K. T. *Int. J. Biochem. Cell Biol.* **2003**, *35*, 22.
8. Casey, B. P.; Glazer, P. M. *Nucleic Acid Res. Mol. Biol.* **2001**, *67*, 163.
9. Knauert, M. P.; Glazer, P. M. *Hum. Mol. Genet.* **2001**, *10*, 2243.
10. Seidman, M. M.; Glazer, P. M. *J. Clin. Invest.* **2003**, *112*, 487.
11. Roig, V.; Asseline, U. *J. Am. Chem. Soc.* **2003**, *125*, 4416.
12. Hildbrand, S.; Blaser, A.; Parel, S. P.; Leumann, C. J. *J. Am. Chem. Soc.* **1997**, *119*, 5499.
13. Xodo, L. E.; Manzini, G.; Quadrifoglio, F.; van der Marcel, G. A.; Van Boom, J. H. *Nucleic Acids Res.* **1991**, *19*, 5625.
14. Carlomagno, T.; Blommers, M. J. J.; Meiler, J.; Cuenoud, B.; Griesinger, C. *J. Am. Chem. Soc.* **2001**, *123*, 7364.
15. Cuenoud, B.; Casset, F.; Hüsken, D.; Natt, F.; Wolf, R. M.; Altmann, K.-H.; Martin, P.; Moser, H. E. *Angew. Chem. Int. Ed.* **1998**, *37*, 1288.
16. Wengel, J. *Acc. Chem. Res.* **1999**, *32*, 301.
17. Obika, S.; Hari, Y.; Sugimoto, T.; Sekiguchi, M.; Imanishi, T. *Tetrahedron Lett.* **2000**, *41*, 8923.
18. Sun, B.-W.; Babu, B. R.; Sørensen, M. D.; Zakrzewska, K.; Wengel, J.; Sun, J.-S. *Biochemistry* **2004**, *43*, 4160.
19. Basye, J.; Trent, J. O.; Gao, D.; Ebbinghaus, S. W. *Nucleic Acids Res.* **2001**, *29*, 4873.
20. Michel, T.; Debart, F.; Heitz, F.; Vasseur, J.-J. *ChemBioChem* **2005**, *6*, 1254.
21. Ehrenmann, F.; Vasseur, J.-J.; Debart, F. *Nucleosides Nucleotides Nucleic Acids* **2001**, *20*, 797.
22. Michel, T.; Debart, F.; Vasseur, J.; Geinguenaud, F.; Taillandier, E. *J. Biomol. Struct. Dyn.* **2003**, *21*, 435.
23. Tereshko, V.; Gryaznov, S. M.; Egli, M. *J. Am. Chem. Soc.* **1998**, *120*, 269.
24. Escudé, C.; Giovannangeli, C.; Sun, J. S.; Lloyd, D. H.; Chen, J.-K.; Gryaznov, S. M.; Garestier, T.; Hélène, C. *Proc. Natl. Acad. Sci. U.S.A.* **1996**, *93*, 4365.
25. Gryaznov, S. M.; L1oyd, D. H.; Chen, J.-K.; Schultz, R. G.; DeDionisio, L. A.; Ratmeyer, L.; Wilson, W. D. *Proc. Natl. Acad. Sci. U.S.A.* **1995**, *92*, 5798.
26. Gryaznov, S. M.; Chen, J.-K. *J. Am. Chem. Soc.* **1994**, *116*, 3143.
27. Chur, A.; Holst, B.; Dahl, O.; Valentin-Hansen, P.; Pedersen, E. B. *Nucleic Acids Res.* **1993**, *21*, 5179.
28. (a) Filichev, V. V.; Pedersen, E. B. *J. Am. Chem. Soc.* **2005**, *127*, 14849; (b) Filichev, V. V.; Gaber, H.; Olsen, T. R.; Jørgensen, P. T.; Jessen, C. H.; Pedersen, E. B. *Eur. J. Org. Chem.* **2006**, 3960; (c) Globisch, D.; Bomholt, N.; Filichev, V. V.; Pedersen, E. B. *Helv. Chim. Acta* **2008**, *91*, 805.
29. Paramasivam, M.; Cogoi, S.; Filichev, V. V.; Bomholt, N.; Pedersen, E. B.; Xodo, L. E. *Nucleic Acids Res.* **2008**, *36*, 3494.

30. Elovaara, E.; Mikkola, J.; Stockmann-Juvala, H.; Luukkanen, L.; Keski-Hynnilä, H.; Kostianinen, R.; Pasanen, M.; Pelkonen, O.; Vainio, H. *Arch. Toxicol.* **2007**, *81*, 169.
31. Chau, A.; Cote, B.; Ducharme, Y.; Frenette, R.; Friesen, R.; Gagnon, M.; Giroux, A.; Martins, E.; Yu, H.; Wu, T. WO 2007/095753, 2007.
32. Kim, B. Y.; Ahn, J. B.; Lee, H. W.; Moon, K. S.; Sim, T. B.; Shin, J. S.; Ahn, S. K.; Hong, C. I. *Chem. Pharm. Bull.* **2003**, *51*, 276.
33. Krebs, F. C.; Spanggaard, H. *J. Org. Chem.* **2002**, *67*, 7185.
34. Nakamura, T.; Sato, M.; Kakinuma, H.; Miyata, N.; Taniguchi, K.; Bando, K.; Koda, A.; Kameo, K. *J. Med. Chem.* **2003**, *46*, 5416.
35. Felsenfeld, G.; Miles, H. T. *Annu. Rev. Biochem.* **1967**, *36*, 407.
36. Liu, K.; Miles, H. T.; Frazier, J.; Sasisekharan, V. *Biochemistry* **1993**, *32*, 11802.
37. Filichev, V. V.; Nielsen, M. C.; Bomholt, N.; Jessen, C. H.; Pedersen, E. B. *Angew. Chem. Int. Ed.* **2006**, *45*, 5311.
38. Zhou, B.-W.; Puga, E.; Sun, J.-S.; Garestier, T.; Hélène, C. *J. Am. Chem. Soc.* **1995**, *117*, 10425.
39. Ren, R. X.-F.; Chaudhuri, N. C.; Paris, P. L.; Rumney, I. S.; Kool, E. T. *J. Am. Chem. Soc.* **1996**, *118*, 7671.
40. Guckian, K. M.; Schweitzer, B. A.; Ren, R. X.-F.; Sheils, C. J.; Paris, P. L.; Tahmassebi, D. C.; Kool, E. T. *J. Am. Chem. Soc.* **1996**, *118*, 8182.